

Improved Modeling of Output Conductance and Cut-off Frequency of Bipolar Transistors

J.C.J. Paasschens*, W.J. Kloosterman*, R.J. Havens*, and H.C. de Graaff†

*Philips Research Laboratories, Prof. Holstlaan 4, 5656 AA Eindhoven, The Netherlands
tel.: +31 40 2742210, email: Jeroen.Paasschens@philips.com

†Delft University of Technology, Department ITS, Delft, The Netherlands

Abstract

The collector epilayer is a crucial element in the behaviour of modern bipolar transistors. Compact models for its description, like the Kull model, are therefore of crucial importance too. We give a Mextram-based improvement to these models for quasi-saturation, and show that the output conductance and the cut-off frequency are much smoother. Apart from ohmic quasi-saturation we also include velocity saturation, which also leads to quasi-saturation (Kirk effect).

1 Introduction

One of the effects that is not adequately described in the widely used Gummel-Poon model is quasi-saturation. Quasi-saturation (i.e. the internal base-collector junction is forward biased, whereas externally it is reverse biased) degrades the performance of the transistor, and is due to either ohmic voltage drop in the epilayer or to a voltage drop caused by velocity saturation (Kirk effect). Many improvements have been suggested over the years. One of the major contributions is the description of ohmic quasi-saturation by Kull et al. [1]. This epilayer model has been incorporated in for instance Mextram [2] and Vbic [3]. The physical basis of the model is sound. However, we will show that in its current implementations it has the disadvantage that it is not very smooth in first and higher derivatives of the current w.r.t. voltages.

We give an improvement to the Kull model that is much smoother. We also include velocity saturation, based on the same principles as in Ref. [2]. This results in a superior description of measurements. As an example we compare to measurements on a high-voltage transistor in which the epilayer description is of crucial importance. This epilayer model will be part of the new Mextram 504 release, but can be implemented also in other models.

In Sec. 2 we analyze the Kull model. In Sec. 3 we show our improvements and the comparison with the Kull model. In Secs. 4 and 5 we add velocity saturation effects and current spreading. Our experimental results are discussed in Sec. 6. In Sec. 7 we describe the charge of the epilayer that is needed for the cut-off frequency description.

2 Analysis of the Kull model

The Kull model [1] gives a good description of the currents and charges in the epilayer, as long as it is quasi-neutral throughout. The current is given in terms of the external and internal base-collector biases V_{BCx} and V_{BCi} . These voltages determine the hole densities p_0 at the base-collector

junction and p_W at the buried layer interface:

$$p_0 = \frac{1}{2} \sqrt{1 + 4 \exp[(V_{BCi} - V_{dc})/V_T]} - \frac{1}{2}, \quad (1)$$

$$p_W = \frac{1}{2} \sqrt{1 + 4 \exp[(V_{BCx} - V_{dc})/V_T]} - \frac{1}{2}. \quad (2)$$

These hole densities are normalised to the epilayer doping level N_{epi} . The parameter V_{dc} is the built-in voltage of the base-epilayer junction and has physically the value $V_{dc} = V_T \ln(N_{epi}^2/n_i^2)$. The current is now defined as

$$I_{epi} = (V_{0W} + V_{BCi} - V_{BCx})/R_{Cv}, \quad (3)$$

$$V_{0W} = V_T \{2p_0 - 2p_W - \ln[(1 + p_0)/(1 + p_W)]\}, \quad (4)$$

where for a 1D model $R_{Cv} = W_{epi}/q\mu_n N_{epi} A_{em}$ is the low-current ohmic resistance of the total epilayer. The expression for the current has indeed ohmic behaviour at low currents. It also describes injection of holes into the epilayer due to quasi-saturation (base-widening, see Fig. 1), in which case the normalised hole density at the base-collector junction p_0 is of order 1 or (much) higher.

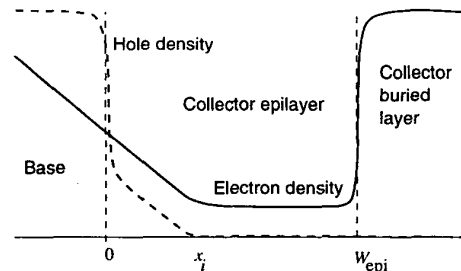


Figure 1: Schematic view of the electron and hole densities in the base-collector region. It also shows the thickness of the epilayer W_{epi} and the injection layer x_i .

Within the Kull model we can calculate the thickness of the injection region

$$\frac{x_i}{W_{epi}} = \frac{V_{0W}}{V_{0W} + V_{BCi} - V_{BCx}}. \quad (5)$$

The epilayer consists of two parts. The first part, between $x = 0$ and x_i , is the injection part, where the hole density is comparable to the electron density. The second part, between $x = x_i$ and W_{epi} is the ohmic part where the hole density is negligible.

Using the equations (3) and (5) we can write

$$V_{BCi} - V_{BCx} = I_{epi} R_{Cv} (1 - x_i/W_{epi}). \quad (6)$$

For low currents, when there is no injection ($x_i = 0$), this equation means that the voltage over the epilayer is just the ohmic voltage drop.

For high currents there is an injection region. Equation (6) implies that the complete voltage drop over the epilayer is just the ohmic voltage drop over the non-injected part ($x > x_i$) of the epilayer. This means that the voltage drop over the injection region is zero, or at least small. This can be understood when we realize that the internal base-collector bias approximately equals V_{dc} , rather independent of the current. This behaviour can be seen in Fig. 2 which shows the V_{BCi} as function of the current I_{epi} for fixed V_{BCx} . A small change in V_{BCi} results already in a large change in p_0 , in V_{0W} , and hence in I_{epi} .

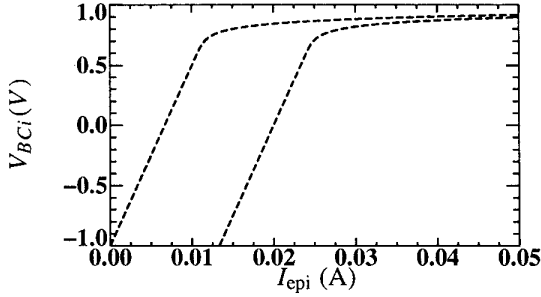


Figure 2: The internal base-collector bias V_{BCi} as function of the current I_{epi} for $V_{BCx} = -1, -3$ V.

Note that there is an abrupt onset of injection (this is the point where V_{BCi} becomes of the order of V_{dc} , or when x_i/W_{epi} starts to rise as in Fig. 3). This leads to incorrect higher derivatives of the current, which can for instance be observed in distortion analysis. The parameters we used come from the experimental results of section 6.

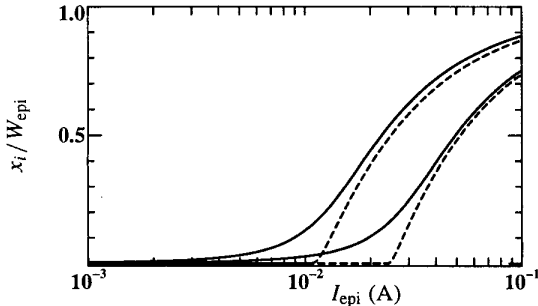


Figure 3: The normalised thickness of the injection region x_i/W_{epi} as function of the current I_{epi} for $V_{BCx} = -1, -3$ V. Dashed line: Kull model Eq. (5). Solid line: our model Eq. (10).

3 Improvement of the Kull model

To improve the smoothness of the formulation we reverse the order of the calculations in the Kull model. For fixed external base-collector bias we assume that the current I_{epi} is given instead of the internal base-collector bias V_{BCi} . From the current and from V_{BCx} we calculate the thickness

x_i of the injection region and from that the internal base-collector bias. We use basically the same equations as the Kull model. Hence we describe the same physics. The internal bias is used for further calculations of for instance the (reverse) main current in the base and the base charge, just as in other bipolar compact models.

3.1 Calculation of the thickness x_i

We use Eq. (6) to calculate the thickness of the injection region. When $x_i > 0$ we know that $V_{BCi} \simeq V_{dc}$. In that case we can write

$$\frac{x_i}{W_{epi}} = 1 - \frac{V_{dc} - V_{BCx}}{I_{epi} R_{Cv}}. \quad (7)$$

In Ref. [4] a similar expression is used. Equation (7) can only be used when $I_{epi} > I_{qs}$, with

$$I_{qs} = (V_{dc} - V_{BCx})/R_{Cv}. \quad (8)$$

The current I_{qs} is the current through the epilayer at the onset of quasi-saturation. To use Eq. (7) also for currents below I_{qs} we replace I_{epi} by \tilde{I} where

$$\tilde{I} = I_{qs} \frac{1 + a_{xi} \ln\{1 + \exp[(I_{epi}/I_{qs} - 1)/a_{xi}]\}}{1 + a_{xi} \ln\{1 + \exp[-1/a_{xi}]\}}. \quad (9)$$

The parameter a_{xi} has a smoothing purpose. Our experience is that it should be of order 0.3 for Si homojunction transistors, and possibly less for heterojunction processes like SiGe. When $I_{epi} \gg I_{qs}$ we have $\tilde{I} \simeq I_{epi}$, as desired. Observe that \tilde{I} is always larger than I_{qs} , unless $I_{epi} = 0$, in which case we have $\tilde{I} = I_{qs}$. The thickness of the injection region x_i is now calculated using Eq. (7) or by solving

$$\tilde{I} = \frac{V_{dc} - V_{BCx}}{R_{Cv} (1 - x_i/W_{epi})}, \quad (10)$$

for given V_{BCx} and I_{epi} . This equation, as well as the expression for I_{qs} , will be improved later-on to include velocity saturation effects.

In Fig. 3 we have shown the result for x_i/W_{epi} . Note that our result indeed shows a much smoother onset of quasi-saturation than the Kull result. By changing a_{xi} one can influence the abruptness by which x_i/W_{epi} starts to increase.

3.2 The internal base-collector bias

Next we need to calculate the internal base-collector bias via the hole density p_0 . To this end we combine Eqs. (3) and (5) to get

$$I_{epi} R_{Cv} x_i/W_{epi} = V_{0W}, \quad (11)$$

where V_{0W} is given in Eq. (4). From this equation we can not calculate p_0 directly. We therefore approximate it with the following

$$I_{epi} R_{Cv} x_i/W_{epi} = 2 V_T (p_0 - p_W) \frac{p_0 + p_W + 1}{p_0 + p_W + 2}. \quad (12)$$

This approximation does not differ more than 5% from the original equation for V_{0W} over the whole range of p_0 and p_W values. Using this second order equation we can now calculate p_0 from p_W , I_{epi} and x_i/W_{epi} . The internal base-collector bias can be found from

$$V_{BCi} = V_{dc} + V_T \ln[p_0 (p_0 + 1)]. \quad (13)$$

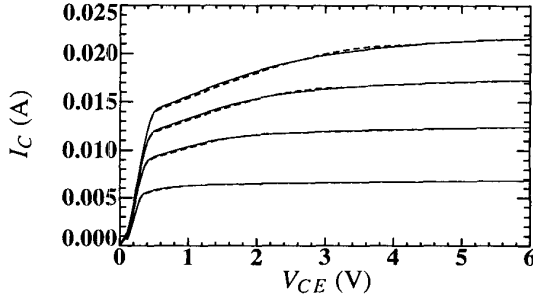


Figure 4: Output characteristic for both the Kull model (dashed line) and our model (solid line) in the ohmic case. $I_B = 50 \mu\text{A}$, $100 \mu\text{A}$, $150 \mu\text{A}$, and $200 \mu\text{A}$.

To compare the results of models for the epilayer one needs to embed them in a complete compact model. The epilayer model described here (including velocity saturation effects described in the next section) will be part of the new version 504 of Mextram. A test version has been implemented in our in-house simulator Pstar. Keeping the rest of the model the same and changing only the model for the epilayer we are able to give a realistic comparison between the Kull model and our new model. The results for the output characteristics are given in Figs. 4 and 5 for the ohmic case. As one can see the difference in the collector current is negligible. There is a much larger difference when we look at the output conductance. In the Kull model one can see a kink when quasi-saturation sets in. In our new model quasi-saturation is present also but its onset is not as abrupt. We will see that the same holds for measurements. For higher derivatives the difference between the two models becomes even larger.

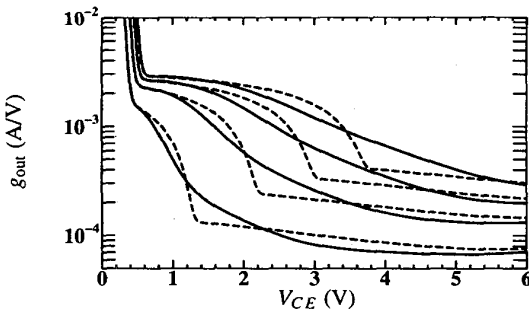


Figure 5: Output conductance $g_{\text{out}} = dI_C/dV_{CE}$ corresponding to Fig. 4. Note the kink at the onset of quasi-saturation in the Kull model.

4 Velocity saturation effects

The equations we presented above hold only when velocity saturation in the epilayer does not play a role. This is true for currents smaller than the hot carrier current $I_{hc} = qN_{\text{epi}}A_{\text{em}}v_{\text{sat}}$, with v_{sat} the saturated drift velocity. For larger currents we need another way of expressing the voltage drop over the non-injection region. Note that the assumption made in Ref. [1] of quasi-neutrality does not hold anymore in the region $x > x_i$. The Kull model is therefore inadequate to describe quasi-saturation due to the Kirk effect.

For large currents ($I \gg I_{hc}$) the space charge resistance $\text{SCR}_{Cv} = W_{\text{epi}}^2/2\varepsilon v_{\text{sat}}A_{\text{em}}$ determines the voltage drop, instead of the ohmic resistance R_{Cv} . For intermediate currents we need a weighted average of both resistances. Using an interpolation like that of Ref. [2, Eq. (19)] we find for the current at the onset of quasi-saturation ($x_i = 0$)

$$I_{qs} = \frac{V_{dc} - V_{BCx}}{\text{SCR}_{Cv}} \times \frac{V_{dc} - V_{BCx} + I_{hc} \text{SCR}_{Cv}}{V_{dc} - V_{BCx} + I_{hc} R_{Cv}}. \quad (14)$$

The current \tilde{I} is still given by Eq. (9). When there is injection, the resistances must be corrected since the non-injected region becomes smaller. Similar to Eq. (10) we now find, defining $y_i = 1 - x_i/W_{\text{epi}}$, the equation

$$\tilde{I} = \frac{V_{dc} - V_{BCx}}{\text{SCR}_{Cv} y_i^2} \times \frac{V_{dc} - V_{BCx} + I_{hc} \text{SCR}_{Cv} y_i^{n+1}}{V_{dc} - V_{BCx} + I_{hc} R_{Cv} y_i^n}, \quad (15)$$

with $n = 1$. This leads to a third order equation for y_i or x_i . This equation can be solved and an explicit formula can be given. We have found however that we can simplify it to a second order equation without loss of accuracy, by taking $n = 0$. This is easier for the implementation in a circuit simulator. Using the thickness x_i we calculate p_0 and the internal base-collector bias from Eqs. (12) and (13). This means that our description of the injection region ($x < x_i$) is not influenced by velocity saturation.

Note that in the limit $I_{hc} \rightarrow \infty$ we get the ohmic result back from the previous section. In the other limit $I_{hc} \rightarrow 0$ we get $\tilde{I} = (V_{dc} - V_{BCx})/[\text{SCR}_{Cv} (1 - x_i/W_{\text{epi}})^2]$. The relation between the current and the thickness of the injection region is now quadratic instead of linear, as in Eq. (6).

5 Current spreading

The derivation we have given above contains the same physics as the Kull model [1] for the ohmic case or the previous Mextram model [2] when including velocity saturation. Up to now it is a one-dimensional model. To take current spreading into account the most important change is due to the fact that the three high current parameters no longer have their one-dimensional value. Instead they get an effective value, as described in [2].

6 Results

To compare our model with measurements we used a $0.6 \times 5.4 \mu\text{m}^2$ NPN-transistor from a 12 V BiCMOS process. The DUT contains 5 transistors in parallel. This transistor has been characterised completely for the CMC benchmarking effort [5], including temperature scaling. The epilayer parameters are: $V_{dc} = 0.68 \text{ V}$, $R_{Cv} = 150 \Omega$, $\text{SCR}_{Cv} = 1250 \Omega$, $I_{hc} = 4 \text{ mA}$, and $a_{xi} = 0.3$. Results of the output characteristics are shown in Figs. 6 and 7.

As one can see the current is modeled well, although the current densities are already high (as can be seen from Fig. 8). Also the output conductance is described reasonably accurate. Neither in the measurements nor in the model do we see a kink such as described by the Kull model in Fig. 5.

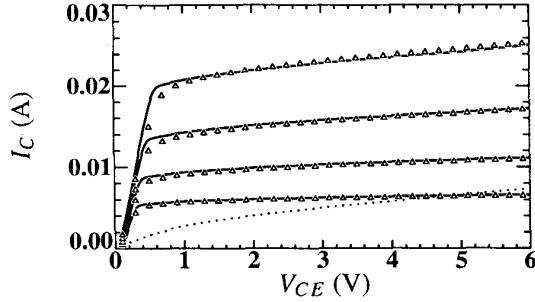


Figure 6: Collector current for $I_B = 50 \mu\text{A}$, $100 \mu\text{A}$, $200 \mu\text{A}$, and $400 \mu\text{A}$. Markers are measurements, lines are the model. The dotted line shows the current I_{qs} , which is almost independent of the base current. For currents above I_{qs} the transistor is in quasi-saturation.

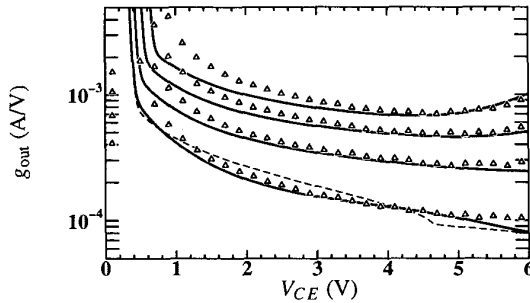


Figure 7: Output conductance $g_{out} = dI_C/dV_{CE}$ corresponding to Fig. 6. The dashed curve shows the result from the old epilayer model for the $I_B = 50 \mu\text{A}$.

7 The epilayer charge

For a complete description we also need an expression for the charge in the epilayer. To calculate it we use the Moll-Ross relation that is used in many models for the current in the quasi-neutral base. Here we use it for the injection region:

$$I_{epi} = I_s \left(e^{V_{bc1}/V_T} - e^{V_{bc2}/V_T} \right) Q_{B0}/Q_{epi}. \quad (16)$$

The saturation current I_s and the zero-bias base hole charge Q_{B0} are either parameters of the intrinsic model or can be calculated from other DC parameters. We can rewrite the equation using Eqs. (1), (2), and (12) to get an expression for Q_{epi}

$$Q_{epi} = \tau_{epi} \frac{2V_T}{R_{Cv}} \frac{x_i}{W_{epi}} (p_0 + p_W + 2), \quad (17)$$

$$\tau_{epi} = I_s Q_{B0} \left(\frac{R_{Cv}}{2V_T} \right)^2 e^{V_{dc}/V_T} = \frac{W_{epi}^2}{4D_n}. \quad (18)$$

Flexibility is enhanced when τ_{epi} is made a parameter itself, instead of being a function of DC parameters.

In quasi-saturation the expression for the epilayer charge becomes $Q_{epi} \approx \tau_{epi} (x_i/W_{epi})^2 I_{epi}$. This equation was first given in Ref. [6] and is used in Ref. [4]. We use the full expression (17) for the charge because it also describes the charge in the case of hard saturation (where the current is small) as well as in reverse mode.

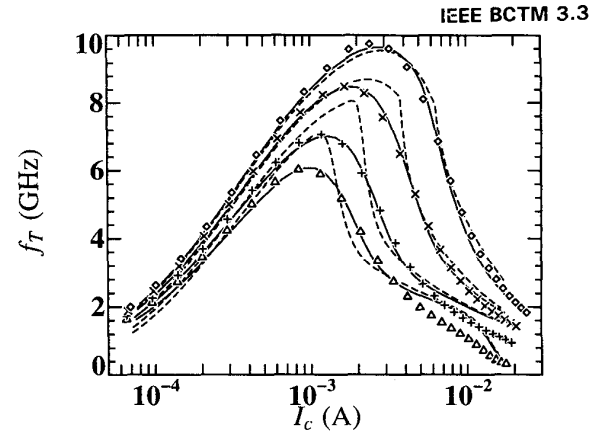


Figure 8: Cut-off frequency f_T for $V_{CE} = 0.5, 0.8, 2.0, 5.0 \text{ V}$ (bottom to top). Markers are measurements, solid lines are from the new epilayer model, and dashed lines are from the old epilayer model.

With the expression for the charge we can calculate the cut-off frequency f_T , shown in Fig. 8. The cut-off frequency f_T is related to the total transit time $\tau_T = dQ/dI_C$. Since in the old epilayer model the collector current is not very smooth (as can be seen from its first derivative g_{out}) one cannot expect the cut-off frequency to be very smooth either. This can indeed be observed in the plot of f_T . Also the improvement can be observed.

8 Summary

We have given a compact model for the behaviour of the collector epilayer of a bipolar transistor. It includes base-widening and quasi-saturation due to an ohmic voltage drop as well as due to the Kirk effect. The excess charge is also described.

We have shown that compared to, for instance, the Kull model it gives a much smoother behaviour, which can already be seen in the first derivatives like g_{out} and f_T . Smoothness is particularly important for higher derivatives which determine the distortion behaviour. The new model is in very good agreement with experiments.

The epilayer model will be part of a new Mextram 504 release, but can be implemented also in other models.

References

- [1] G.M. Kull, L.W. Nagel, S.-W. Lee, P. Lloyd, E.J. Prendergast, and H. Dirks, "Unified circuit model for bipolar transistors including quasi-saturation effect," *IEEE Trans. Elec. Dev.*, **ED-32** (1985) 1103–1113.
- [2] H.C. de Graaff and W.J. Kloosterman, "Modeling of the collector epilayer of a bipolar transistor in the Mextram model," *IEEE Trans. Elec. Dev.*, **ED-42** (1995) 274–282. See also http://www.semiconductors.philips.com/Philips_Models.
- [3] C.C. McAndrew *et al.*, "VBIC95, the vertical bipolar inter-company model," *J. Solid-State Circ.*, **31** (1996) 1476–1483.
- [4] M. Schröter and T.-Y. Lee, "Physics-based minority charge and transit time modeling for bipolar transistors," *IEEE Trans. Elec. Dev.*, **ED-46** (1999) 288–300.
- [5] For the Compact Model Council bipolar standardisation effort see <http://www.eigroup.org/cmc>.
- [6] J.R.A. Beale and J.A.G. Slatter, "The equivalent circuit of a transistor with a lightly doped collector operating in saturation," *Solid State Elec.*, **11** (1968) 241–252.